LBL-31333
UC-403, 820

Lawrence Berkeley Laboratory
UNIVERSITY OF CALIFORNIA

EARTH SCIENCES DIVISION

Presented at the Third International Reservoir Characterization Technical Conference, Tulsa, OK, November 3–5, 1992, and to be published in the Proceedings

Modeling Heterogeneous and Fractured Reservoirs with Inverse Methods Based on Iterated Function Systems

J.C.S. Long, C. Doughty, K. Hestir, and S. Martel

May 1992

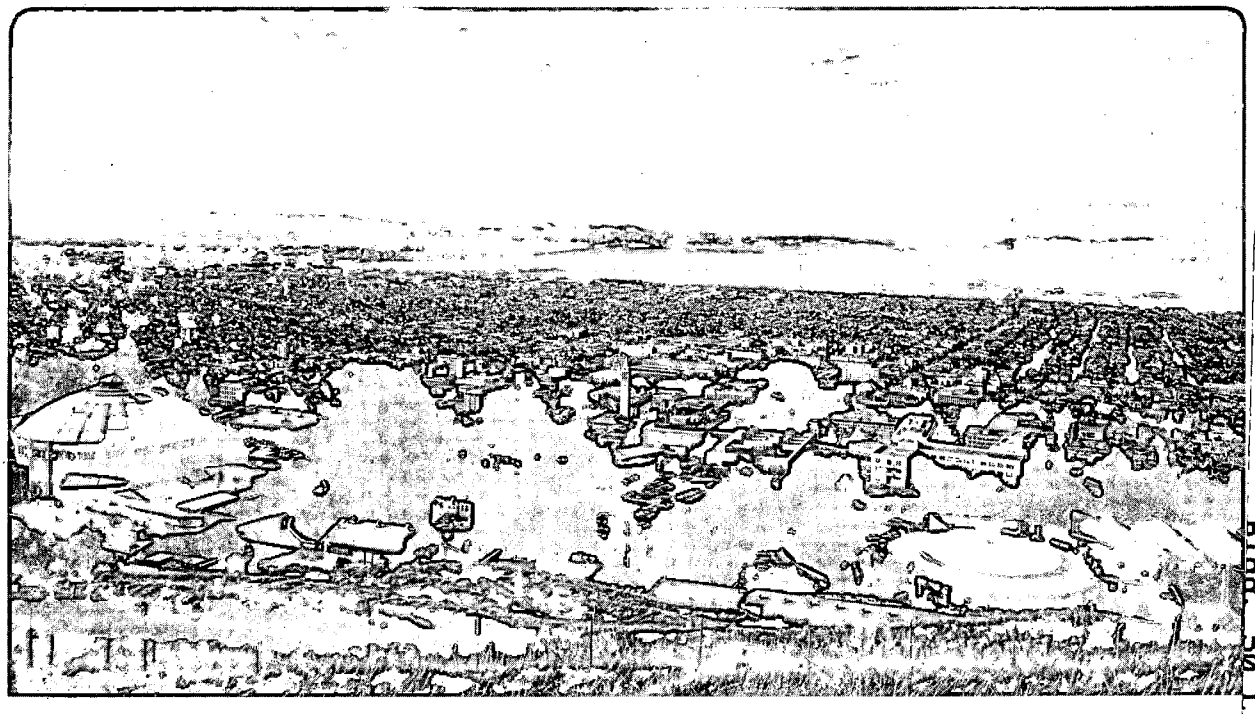

Prepared for the U.S. Department of Energy under Contract Number DE-AC03-76SF00098

DISCLAIMER

LBL-31333

Modeling Heterogeneous and Fractured Reservoirs with Inverse Methods Based on Iterated Function Systems

Jane C. S. Long, Christine Doughty, Kevin Hestir, and Stephen Martel

Earth Sciences Division
Lawrence Berkeley Laboratory
University of California
Berkeley, California 94720

May 1992

This work was supported by the Director, Office of Civilian Radioactive Waste Management, Office of External Relations, and by the Director, Office of Energy Research, Office of Health and Environmental Research, Ecological Research Division, Subsurface Science Program, of the U.S. Department of Energy under Contract No. DE-AC03-76SF00098.

Modeling Heterogeneous and Fractured Reservoirs with Inverse Methods Based on Iterated Function Systems

Jane C. S. Long, Christine Doughty,
Kevin Hestir and Stephen Martel

Earth Sciences Division
Lawrence Berkeley Laboratory
Berkeley, CA 94720

ABSTRACT

Fractured and heterogeneous reservoirs are complex and difficult to characterize. In many cases, the modeling approaches used for making predictions of behavior in such reservoirs have been unsatisfactory. In this paper we describe a new modeling approach which results in a model that has fractal-like qualities. This is an inverse approach which uses observations of reservoir behavior to create a model that can reproduce observed behavior. The model is described by an iterated function system (IFS) that creates a fractal-like object that can be mapped into a conductivity distribution. It may be possible to identify subclasses of Iterated Function Systems which describe geological facies. By limiting the behavior-based search for an IFS to the geologic subclasses, we can condition the reservoir model on geologic information. This technique is under development, but several examples provide encouragement for eventual application to reservoir prediction.

1.0 INTRODUCTION

Most of the established techniques for modeling heterogeneous and fractured reservoirs are based on the assumption that the reservoir acts as an equivalent continuum on some scale, often called the representative elementary volume (REV) (Toth, 1967). Further, a common assumption is that the reservoir can be modeled by tesselating the entire region of interest with blocks of equivalent continua that are at least as large as the REV. However, it has become increasingly apparent that reservoir heterogeneities occur on every scale (Freeze, 1975), and that the concept of the REV may not always be appropriate. For example, in a fractured rock, we find fractures on every scale from the microfracture to major fault. Dominant flow paths develop where open, conductive fractures intersect. Flow may completely bypass parts of the reservoir and

connected regions may be complex and hard to define. A similar case may be made for sand-body reservoirs. In these cases, it is difficult to define a heterogeneous model for reservoir behavior.

Two modeling approaches are commonly used to include the effect of heterogeneities. (For this discussion we can consider fractures as just another type of heterogeneity.) The first approach we will call the "forward" approach. In this approach one tries to infer the distribution of heterogeneities and the spatial relationships from conductivity measurements. Tools such as geostatistics can be used to create realizations which match both the local measurements and the inferred spatial correlation. The primary difficulty with this approach is that such models rely on an estimate of the geometry of the heterogeneities to predict the behavior. A model which reproduces the geometry may not match observed behavior, much less correctly predict new behavior (Long et al., 1991). Secondly, most of these techniques are restricted to producing smooth models of heterogeneities. Physical systems that are highly convoluted or poorly connected such as meander belts or fracture networks, may be extremely difficult to simulate with geostatistics.

The second approach is the inverse method. In this approach we search for a pattern of heterogeneity which matches the observed behavior of the reservoir, usually observed heads under assumed steady flow conditions. Such models have been developed by Carrera and Neuman (1986a,b,c) and Kitanidis and Vomvoris (1983), for example. The latter is particularly interesting because the inversion method is used to determine a relatively small set of geostatistical parameters, which are then used to generate heterogeneous hydrologic property distributions via kriging.

In the inverse techniques we have developed at Lawrence Berkeley Laboratory, we search for equivalent models which are based on a geologic understanding of flow. For example, Simulated Annealing (Davey et al., 1989) is an inversion technique that has been applied to fractured rock to find an Equivalent Discontinuum model (Long et al., 1991). Simulated Annealing is applied to a partially filled lattice of one-dimensional conductors, called a template, which is in effect a geologically based conceptual model for the fracture system. The algorithm searches for a configuration of lattice elements which can reproduce observed hydrologic data. At each iteration, one calculates the "energy," E, of the configuration, which is a function of the difference between model predictions and observed behavior. Then a random change is made in the lattice and the new energy is computed and compared to the old energy. If the energy is decreased, the change in the configuration is kept. If the energy is increased by the change, the choice of whether or not to keep the new configuration is made randomly based on a probability which decreases with the amount of energy increase, allowing the algorithm to "wiggle" out of local minima. Use of the annealing algorithm is more completely documented by Davey et al. (1989) and Long et al. (1991).

The Iterated Function System (IFS) inversion method described in this paper is similar to the application of Simulated Annealing to Equivalent

Discontinuum models. An IFS is used to create a fractal-like object (an attractor) which describes reservoir heterogeneities or fractures. The inverse analysis optimizes the parameters of the IFS until the attractor-based hydrologic model matches the observed behavior of the hydraulic data.

Below we briefly describe the IFS concept and explain how these functions are used in an inversion. Then we discuss the well test data that can be used in an inversion. We provide two examples of inversions based on synthetic data generated from numerical models and two preliminary field based examples, one for heterogeneous porous materials and one for fractured rock. A third preliminary example shows how we might find classes of IFS which produce fracture geometries similar to those observed in nature. Finally we discuss future directions.

2.0 ITERATED FUNCTION SYSTEMS

An iterated function system (IFS) is a standard way to model self similar geometrical structures (Barnsley, 1988) which was developed for use in computer graphics in order to find efficient means for storing the information describing each pixel of a complex picture. In this application, one identifies an iterative process that will create the picture rather than storing the information for each pixel. The iterative process is defined by an IFS which has a relatively small number of parameters. The use of an IFS essentially exchanges the use of computer storage for the use of computer time. In our application, we want to create a model of a complex heterogeneous geologic system. Instead of trying to describe this system "pixel by pixel," we look for an IFS that can describe the geometry of the system with a small number of parameters.

An IFS creates a picture starting with an initial set of points and a set of iterative functions. At each iteration, each function in the system operates on the set of points and according to the parameters in the function translates, reflects, rotates, contracts or distorts the set of points. Over many iterations, the points in the picture coalesce towards an "attractor" which is a fractal-like object. The shape of this attractor changes gradually when the parameters of the IFS gradually change.

To create an IFS one first specifies a function f, which maps sets to sets:

$$f(A_0) = A_1 \tag{2.1}$$

where A_0 and A_1 are (compact) subsets of two (or three) dimensional space. A set A_∞ can then be defined by

$$A_{n+1} = f(A_n) \quad n = 0, 1, \ldots \tag{2.2}$$

$$A_\infty = \lim_{n\to\infty} A_n \ .$$

Given certain restrictions on the set function f, one can show (Barnsley 1988) that A_∞ exists, is independent of the starting set A_0, and generally has a fractional Hausdorff dimension. Hence f determines a fractal, A_∞. If we have a

function f that is easily parameterized, then the fractal A_∞ is parameterized as well. This leads to a nice setup for modeling real-world problems, because a small number of parameters can be used to characterize a complex geometry.

A wide variety of Iterated Function Systems can be defined, but they fall into two main categories: deterministic and probabilistic. A deterministic IFS has uniquely determined parameters, and thus creates a unique attractor A_∞. A random IFS chooses some or all of its parameters randomly from probability distributions, so multiple realizations of A_∞ differ. The Iterated Function Systems used in the hydrologic inversions given in this paper are deterministic and of the form of Equations (2.3) and (2.4); those used in the fracture growth scheme (Section 8) are random.

One important example of a deterministic f used extensively by Barnsley (1988) is:

$$f(A) = g_1(A) \cup g_2(A) \cup \ldots g_k(A) \ . \tag{2.3}$$

Here the g_i's are so called affine transforms:

$$g_i(A) = \bigcup_{\vec{x} \in A} g_i(\vec{x}) \tag{2.4}$$

$$g_i(\vec{x}) = B_i\vec{x} + \vec{b}_i$$

where B_i is a matrix and $\vec{b}_i$ a vector. The parameters characterizing f are the entries in the B_i's and $\vec{b}_i$'s. The matrix, B_i, serves to rotate, reflect, distort, and contract and the vector, $\vec{b}_i$, translates. An example IFS using k = 3 affine transformations which contract and translate, resulting in a fractal called a Sierpinski's gasket, is shown in Figure 2.1. The IFS is specified by

$$B_1 = B_2 = B_3 = \begin{bmatrix} 0.5 & 0.0 \\ 0.0 & 0.5 \end{bmatrix}, \tag{2.5}$$

$$\vec{b}_1 = (0.0, 0.0) \ , \quad \vec{b}_2 = (0.5, 0.0) \ , \quad \vec{b}_3 = (0.0, 0.5) \ .$$

Figure 2.2 shows the attractors generated by a sequence of functions $f_1, f_2, \cdots, f_6$, where f_1 is the Sierpinski's gasket, and for j = 2, 6 every parameter of f_j differs from the corresponding parameter of f_{j-1} by a small increment. The continuous change in parameters is manifested as a continuous change in the attractors, which is a useful but not necessary condition for an IFS-based inversion procedure to work.

The most general affine transforms that operate in two-dimensions have four arbitrary entries in each B_i matrix, and two arbitrary values in each $\vec{b}_i$ vector, which gives a total of 6 parameters for each affine transformation. By understanding how the different parameters affect the shape of the attractor, we can constrain parameters to produce attractors that have desired properties, for example mimicking certain geological facies. As well as making the inversion procedure more efficient by reducing the dimensionality of the parameter space,

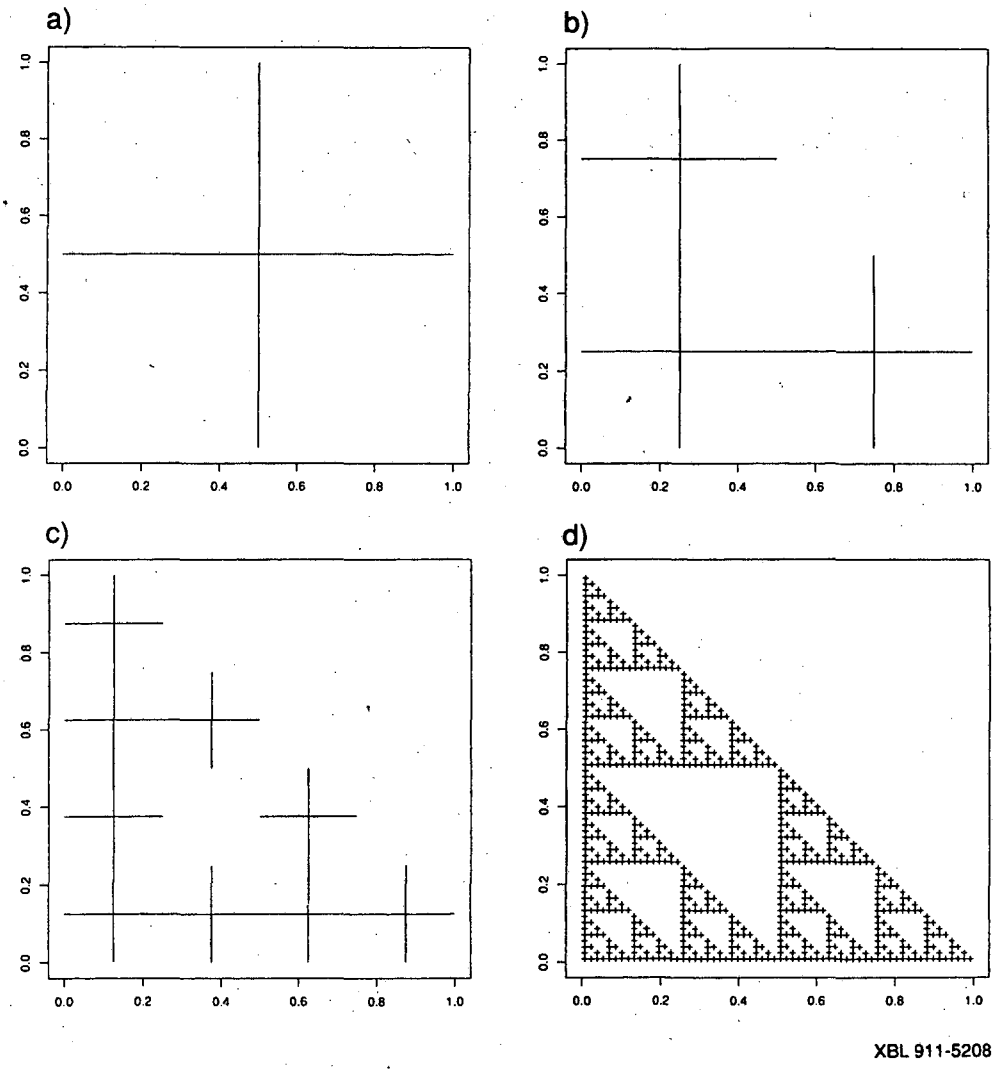

Figure 2.1. Generation of a Sierpinski's gasket using three affine transformations.

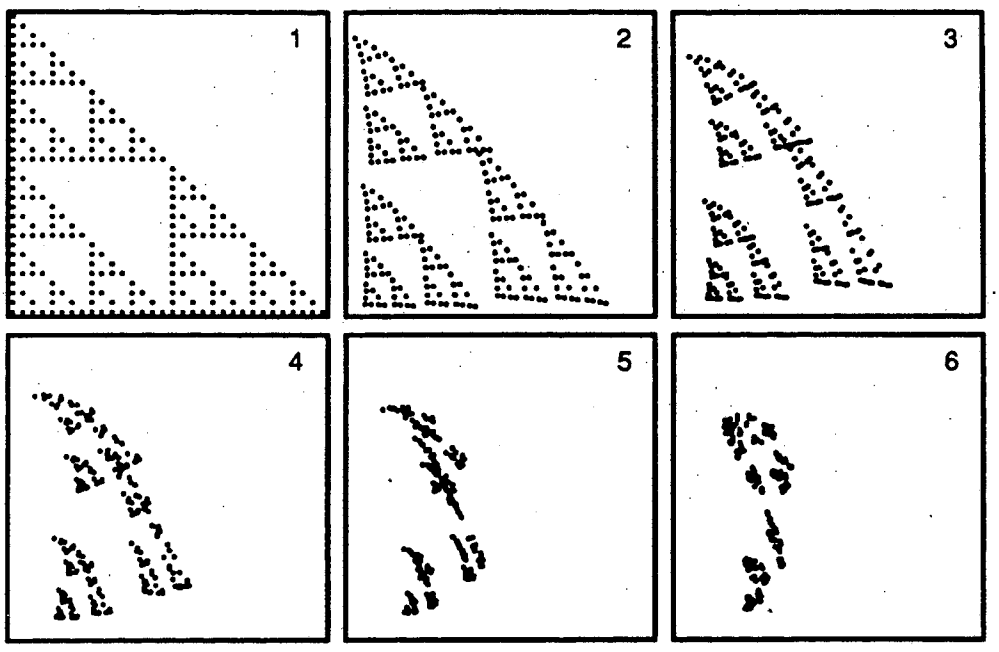

Figure 2.2. A series of attractors generated by functions whose parameters differ by small increments.

these constraints make the inversion more robust by conditioning it on known geological conditions. One simple example is to construct each B_i as a rotation matrix

$$B = S\begin{bmatrix}\cos\theta & -\sin\theta \\ \sin\theta & \cos\theta\end{bmatrix} \tag{2.6}$$

where S is a contractivity factor ($0 < S < 1$) and θ is a rotation angle. This formulation reduces the number of parameters of the IFS from 6 to 4 per affine transformation. By restricting θ and $\vec{b}$ to a limited range, directional trends observed in geologic media can be reproduced in the attractors.

3.0 INVERSION BASED ON ITERATED FUNCTION SYSTEMS

To use the IFS as a basis for hydrologic inversions we map the points of the attractor into a hydrologic property (conductivity, storativity etc.) distribution and use the finite element code TRINET (Karasaki, 1987) to simulate a well test. In the examples given here, the finite element mesh consists of a lattice of one dimensional conductors. We superimpose the attractor on the lattice and increment the conductance and storativity of the lattice elements that are close to each point on the attractor, as shown in Figure 3.1. The hydrologic properties of a

lattice element can be incremented as many times as there are points on the attractor near by. In this way the small number of parameters of an IFS define the conductance and storativity distribution for thousands of elements.

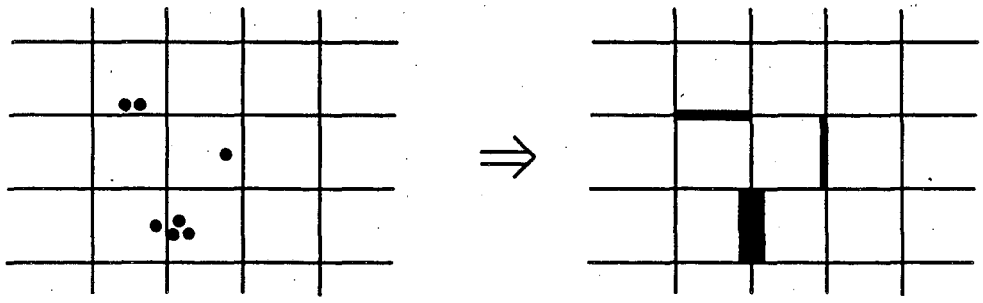

XBL 919-2021

Figure 3.1. "Step" mapping between points on the attractor and increments in hydrologic properties of the lattice.

The inversion algorithm searches for IFS parameters which define a heterogeneous system that behaves like the observed well tests. We first construct a model of the flow system using a lattice of elements modified by an arbitrary IFS. We then optimize the parameters of the IFS until the model produces a good match to the well test data. The match is quantified by the energy, E, which represents, in a single number, the total amount of mismatch between the observed and modeled drawdowns, and is a convenient way of quantifying the "goodness of fit" of the model to the data during the course of an inversion. We define E as

$$E = \sum \left[\ln(h_o) - \ln(h_c) \right]^2 \qquad (3.1)$$

where h_o is the observed head (or drawdown) and h_c is the head (or drawdown) calculated using the hydrologic properties mapped from the attractor. E can also be a function of flow differences or any other pertinent measure of behavior. The sum is taken over a discrete set of observation times and all observation wells. E is not normalized by the number of data points or by the magnitude of the observed drawdowns, so one cannot say *a priori* that a certain value (e.g., E = 10) is "good" or "bad" for all problems. At this point we use judgment to decide whether the mismatch between observed and calculated drawdowns is sufficiently small to be insignificant.

The optimization can be done in a variety of ways. We have used several routines available in standard numerical libraries, including downhill simplex

and direction set methods (Press et al., 1986). One optimization technique that seems to work well is Simulated Annealing. In this case, we randomly choose new values of the IFS parameters and accept or reject these new choices according to the annealing algorithm as described above.

Some parts of the inversion algorithm are arbitrary. For example, we choose the number of affine transforms, k, that make up the IFS. We also choose the number of points, M, for the IFS to use in creating the attractor. The larger M is, the greater the contrast in permeability can be. One could use a high value of M to model highly conductive features in a relatively impermeable matrix or a lower value of M to model conductive features in a slightly impermeable matrix. Further, we also arbitrarily choose how to relate the increment in conductance and storativity represented by each point of the attractor. Another arbitrary choice is exactly how to map the attractor into the hydrologic parameters. One possibility is to modify the properties of just the single element closest to each attractor point (a "step" map). Alternatively, properties for all elements near an attractor could be affected, with the magnitude of the change decreasing as a function of distance from the attractor point (a distributed map). We have just begun to study the effects of such choices.

One of the attractive features of this approach is that it may be possible to choose sub-classes of Iterated Function Systems which tend to produce features observed in a geologic investigation. For example, we may be able to find Iterated Function Systems that always produce a specific type of brittle shear zone or meander belt structure. In these cases we could confine the search for hydrologic behavior to the sub-class of IFS that represents the geology. Along the same lines, once we have identified the form of the IFS that best explains all the data, the model will have fractal-like properties that may help to extrapolate behavior to scales that can not be tested in reasonable time frames.

4.0 HYDROLOGIC DATA FOR INVERSION

One of the significant problems associated with applying these techniques is the choice of data set to invert. In principle, any physical phenomena of interest which can be numerically modeled and also monitored in the field can be used in the inverse method. In practice, it can be quite difficult to pick a good data set for analysis. Some of the difficulties arise from the usual problems with field data: poorly known boundary conditions, incomplete or insufficient data, etc. Another problem faced in the inversion process is comparing model results to data. In the model we choose base values of conductance and storativity. Then, these parameters are incremented using the IFS map and the model is used to simulate well tests. The model results and the data may differ for two reasons: (1) the base values of the parameters are wrong or (2) the distribution of heterogeneities is wrong. The inversion process defined above is only designed to address the second reason. In some cases an incorrect choice of base values can be treated by shifting the model results on a log drawdown – log time plot. The y-shift corresponds to scaling the conductances of the elements uniformly up or down

and the x-shift scales the diffusivity (conductivity divided by storativity). Thus at each iteration, the model results are first shifted to obtain the best fit to the data and then the energy is calculated. However, as discussed below, it is not always appropriate to shift the model results. Further, if the base parameters chosen are very bad estimates, so that large shifts are required, numerical problems can occur. For example, a large over estimate of base conductance can cause drawdowns to be so small that they are swamped by round off errors. A large log-time shift may either cause the temporal resolution of the model to be inadequate at early times, or the period of time modeled to be too short. Although shifting is an elegant way to avoid repetitious modeling, for practical purposes it may be preferable to incorporate the choice of base parameters into the optimization process. Some of the considerations necessary for using different types and amounts of well test data are discussed below.

4.1 Steady-State Tests

The simplest approach has been to use the steady-state head distribution resulting from a pumping test with a constant flow boundary condition applied at the pumping well. The energy function is constructed as a function of the differences between modeled and measured heads or drawdowns. Drawdowns induced by such a test are relatively simple to measure, and steady flow is easy and quick to model, allowing many iterations of the model to be practical. However, for steady-state flow, the pattern of drawdowns does not change when conductances of the medium are uniformly scaled up or down. So, using a single steady-state test will only give a pattern of conductance contrasts which matches the head distribution. The value of these conductances can then be scaled up or down until the applied flow boundary condition is matched. This means, not surprisingly, that models obtained largely by matching drawdowns should be more sensitive predictors of drawdown than they are of flow.

Greater sensitivity to flow can be gained by combining a series of steady-state tests. If constant flow is applied at the pumping well, the energy function can include the head at the pumping well treated as any other observed head. In this case, each of the separate tests is modeled at each iteration and the factor incrementing all the element conductances is chosen to best fit all the flow boundary conditions. If constant head boundary conditions are applied at the pumping well, the energy function can be constructed as an appropriately scaled combination of squared head differences at observation wells and squared flow differences at the pumping well. In this case, no overall scaling of conductances is needed.

Generally, multiple steady tests may provide the best data for inversion because there is no dependence on storage coefficient and the time required for steady flow calculations is very small. However, in the field each steady test is very time consuming and consequently few are usually available.

4.2 Transient Tests

Alternatively, one can use the transient interference data resulting from a constant flow boundary condition. The flow rate used in the field is specified in the model in order to predict the transient drawdown response. At each iteration, the model predicts curves of drawdown versus time that can be shifted in both the x- and y-directions in log-log space until a best match is obtained to the real curves. This process is similar to matching data to a Theis curve but in this case the shift corresponds to scaling the conductances and storage coefficients for the elements in the model. With multiple observation points, it becomes necessary to find the best shift on average. Although this process is conceptually simple, the vagaries of numerical calculation combined with the vagaries of real data can make curve matching extremely difficult to do automatically for thousands of iterations. The energy at each iteration is the sum of the squared differences in log of head for each observation point at selected times. The advantage of using this type of data in inversion is that the transients reflect the distribution of heterogeneities in space, where as a steady test is more likely to reflect the biggest bottle-neck, irrespective of where it is. The disadvantage of transient data is that we are forced to make an assumption about the relationship between storage and conductance; in other words we have more information, but another parameter to specify.

As in the steady-state case, a slightly different procedure must be used if the transient test has a constant head boundary condition. In this case we should use both the transient drawdown data at the observation wells and the transient flow rate at the pumping well in the energy function. Under these conditions the y-shift is not needed because head is pegged by the constant head boundary condition. Consequently, constant head tests are somewhat more sensitive to the initial estimate of the element conductances and in practice are more difficult to invert than constant flow test data.

4.3 Combining Different Types of Tests

If several different tests are available, these can be combined. In principle any combination of steady, transient, constant-flow or constant-head data can be combined. The main drawback for combining a large number of transient tests is the possibility of using an enormous amount of cpu time. The calculation time scales with the number of tests times the number of time steps times the number of iterations. It is not difficult to conceive of a problem that could take on the order of a month to invert.

For multiple constant-flow transients, the procedure is straight forward. At each iteration, each test is modeled and the best-fit x- and y-shifts for all the curves are identified. Theoretically, a steady-state test is a subset of a transient test and the steady drawdowns predicted by the model can be matched to the data by a shift in the y-direction, with the x-shift irrelevant for steady-state conditions. On the other hand, if we include a constant head test (transient or steady-state), we cannot use a y-shift to match the drawdown data from the constant head test.

One approach is not to use the y-shift on any of the drawdown curves. In this case, we need to have a good *a priori* estimate of element conductance. Again, flow data should be included in the energy function for the constant head case.

In general, the inversion of well test data yields a non-unique solution. Fundamentally, one rarely has enough data to specify a unique solution. The advantage of using multiple well tests is that each additional test provides more information about the system. We can use a single well test to predict a second well test, and the first two well tests to predict the third. In this way we can see if our ability to make predictions improves which implies an improvement in the uniqueness of the solution.

5.0 SYNTHETIC EXAMPLES

One way to see how well the inversion algorithm works is to generate synthetic data from a prescribed model and see if the model used to generate the data can be recovered by the inversion. At this point, we have completed a few simple cases which serve to provide encouragement for the concepts as well as point out the limitations of the method. Many issues have not yet been addressed and will be the object of further study.

5.1 A Linear High-Conductivity Feature

The first synthetic case is a simplified model which might represent the hydraulic conditions imposed by a buried stream channel or the trace of a conductive fault. We construct a two-dimensional model with a highly conductive linear feature and use IFS inversion to see if we can find the location of this feature.

An IFS composed of two affine transforms of the form

$$f(A) = g_1(A) \cup g_2(A) \tag{5.1}$$

where

$$g_i(\vec{x}) = \begin{bmatrix} 0.5 & 0.0 \\ 0.0 & 0.5 \end{bmatrix} \vec{x} + \vec{b}_i \tag{5.2}$$

has only four parameters, the two components of each of $\vec{b}_1$ and $\vec{b}_2$. This f always produces a linear attractor, with the length and orientation of the line segment depending on the $\vec{b}_i$'s. A linear high conductivity feature provides a simple demonstration of the IFS inversion procedure for several reasons: The inversion is fast because the dimension of the parameter space is small (4 instead of the usual 6 parameters per affine transformation); the evolution of the attractor as the inversion progresses is easy to visualize; and the linear high conductivity feature has a clear "signature" on the pressure transients, making the inverse problem better posed.

A synthetic data set was generated for a constant flow pump test conducted in a medium with a linear feature that has a conductivity 500 times higher than the background (see Figure 5.1). The central well pumps at a constant rate and

transient heads are calculated for four surrounding observation wells. A two-dimensional finite element mesh composed of a regular 20 by 20 grid of linear elements is used; head is held constant at the outer boundary. Figure 5.2 shows the transient heads calculated for this conductivity distribution (the synthetic data). The effect of the high conductivity feature is clearly seen in the earlier, larger response of the upper well in Figure 5.2.

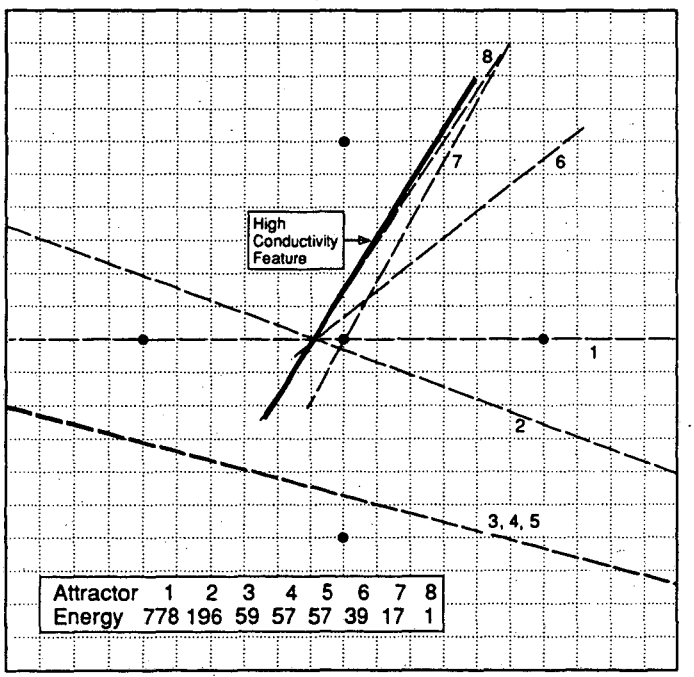

Figure 5.1. Model of synthetic case 1: the heavy black line shows the region of enhanced conductivity, the wells are marked as large black dots, and the mesh is shown as dotted lines. The initial attractor for inversion is the dashed line labeled 1; the dashed lines labeled 2-8 are a sequence of attractors found during the inversion.

The attractors found at various points during the inversion are shown in Figure 5.1, along with the corresponding energies. Note that this figure shows the attractor, each point of which is used to increment the nearest element conductance, not the conductance distribution itself. Figure 5.2 shows the pressure transients for a uniform medium (no attractor, $E = 90$) and for the final attractor determined by the inversion ($E = 1.2$). The small energy of the final attractor is due to the excellent match of all the pressure transients and is not surprising in light of the similarity of the final attractor (labeled 8 in Figure 5.1) to the original high-conductivity feature. This synthetic case illustrates the IFS inversion working very well, but it should be emphasized that real-world problems are likely to be much more complicated.

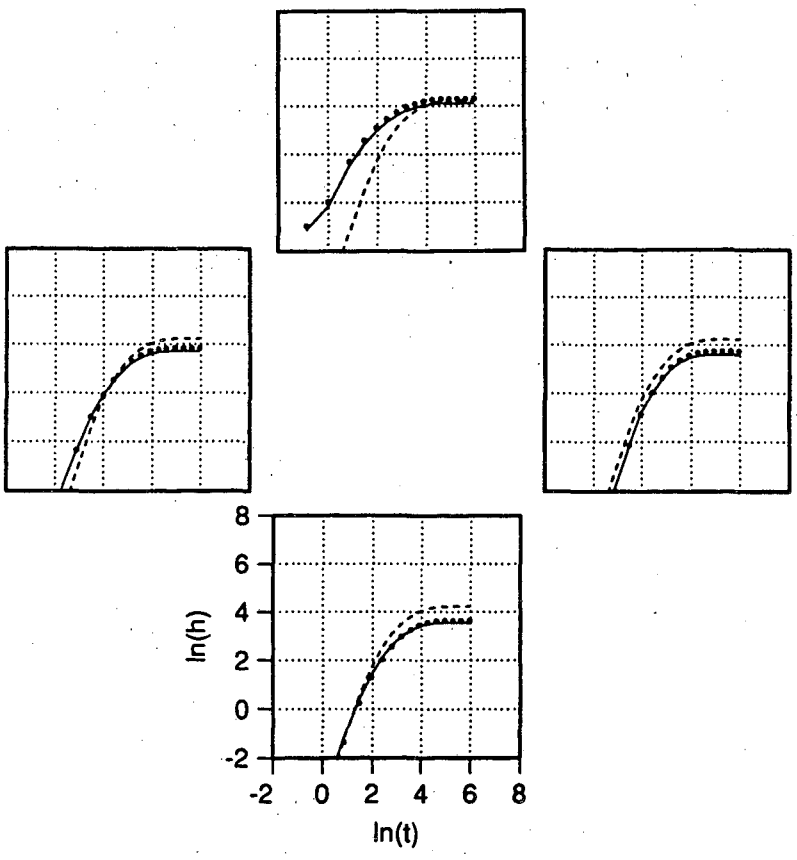

Figure 5.2. Transient heads at the four observation wells for synthetic case 1: data (black dots), a uniform medium with no attractor (dashed lines, E = 90), and the attractor labeled 8 in Figure 5.1 (solid lines, E = 1.2). The arrangement of the plots on the page follows the locations of the observation wells in the well field.

5.2 A Square Zone of Contrasting Conductivity

A second synthetic case consists of a central square region with hydrological properties significantly different than the surrounding region (Figure 5.3). First we allowed the center region to have a conductivity and storativity 100 times higher than the outer region. Then, we reversed these ratios. In each case, interference data was generated by pumping from well 0 and monitoring the response at the other five side and corner wells. The five drawdown vs. time curves are inverted using Simulated Annealing to find an optimal IFS composed of three affine transforms.

The IFS chosen to provide a starting point for the inversion is the Sierpinski's gasket shown in the first frame of Figure 2.2.

Figure 5.4 shows two different solutions for the inversion with the high conductivity and storativity in the center. Figure 5.5 shows the match between the synthetic well test data and the model results for the first solution. Figures 5.6

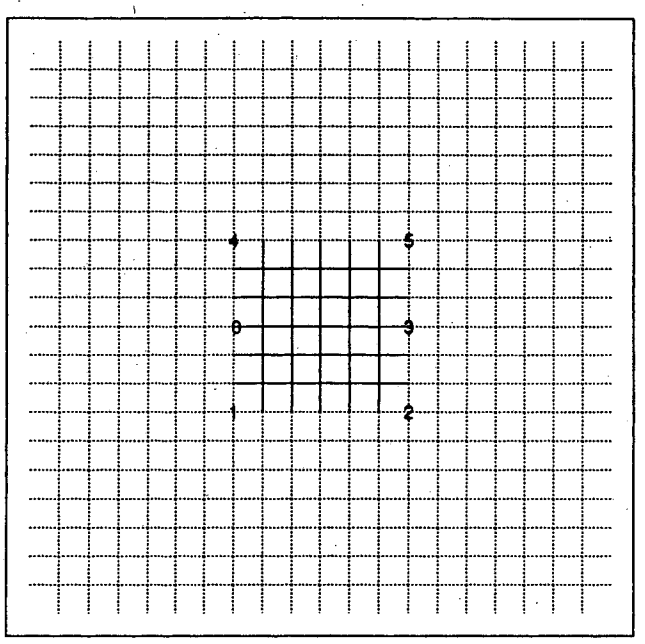

Figure 5.3. Model for the second synthetic case. The central region is at first 100 times more conductive than the outer region, then 100 times less conductive. The numbers show the locations of six wells.

and 5.7 show the corresponding information for the low conductivity and storativity in the center. The energy associated with a homogeneous lattice is about E = 200 and the energy of all the IFS solutions is about E = 10.

The algorithm is clearly able to find a central high conductivity zone and this is very encouraging. This case should be extended to see how large a contrast and how small an inhomogeneity can be detected. Also, we should investigate how far away the wells can be from the anomaly and still detect it.

Interestingly, the reverse case does not recover the geometry of the original model as well. When the high conductivity is on the outside, the algorithm puts a small region of high conductivity on the outside, but does not spread it around the anomaly. We suspect that if we based the inversion on a combination of well tests from different wells, we would have a better chance to resolve the anomaly. Also, we could use the attractor to decrement the conductance instead of increment it. This may give a solution similar to the case above.

5.3 Conclusions Drawn from Synthetic Cases

The synthetic cases we have conducted so far have provided some general confidence in the approach we are taking and show that an extensive study of synthetic cases is warranted to help refine the algorithm. Furthermore, it will be useful to corrupt the synthetic data by adding noise or by varying the boundary conditions to see how best to develop robust inversion techniques.

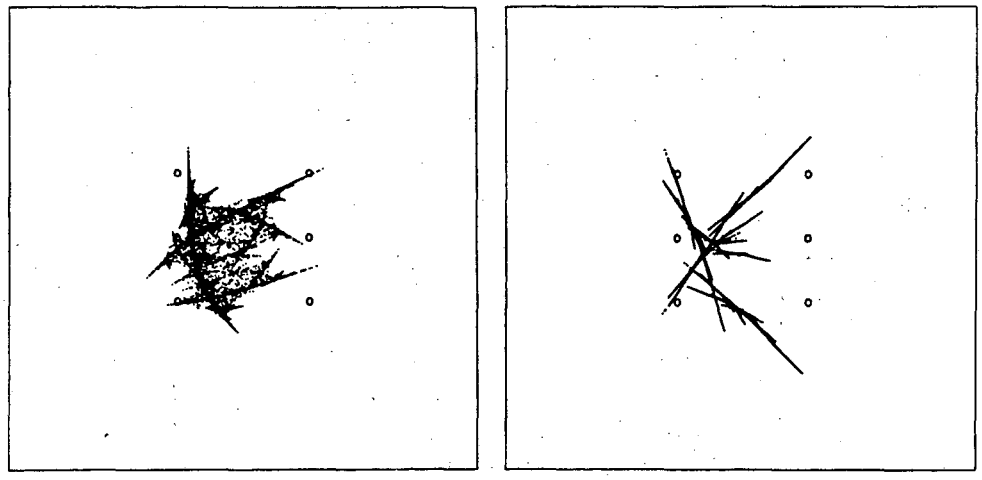

Figure 5.4. Two different attractors found by inversion of the second synthetic case for the high conductivity in the center.

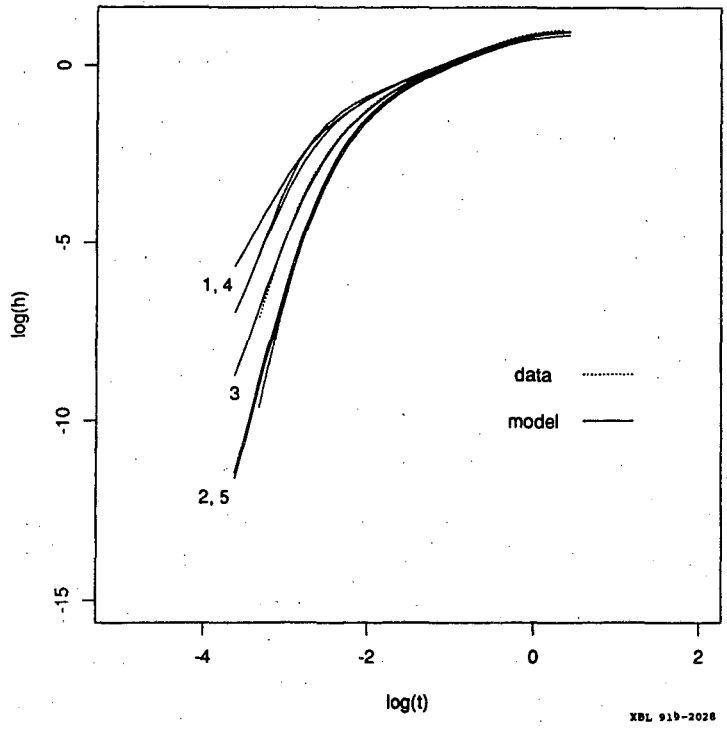

Figure 5.5. Transient drawdown response for the second synthetic case for the high conductivity in the center.

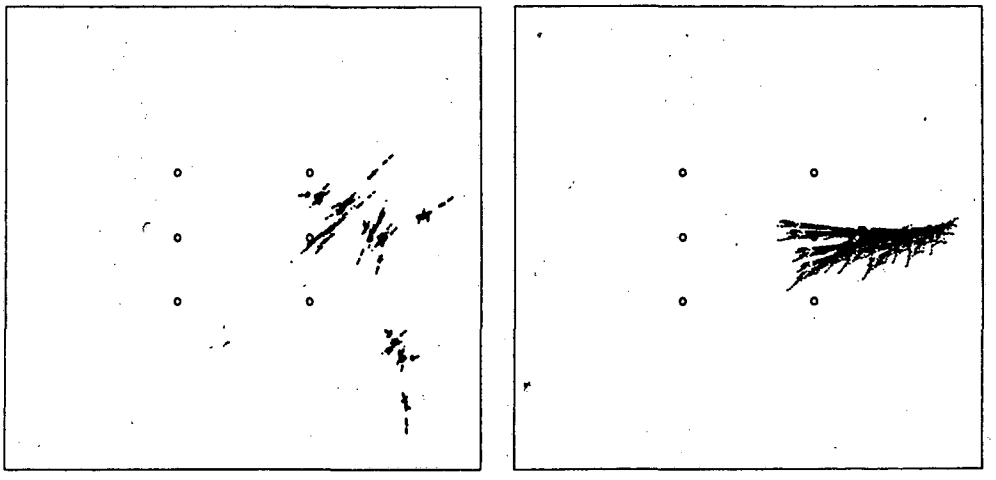

Figure 5.6. Two different attractors found by inversion of the second synthetic case for the low conductivity in the center.

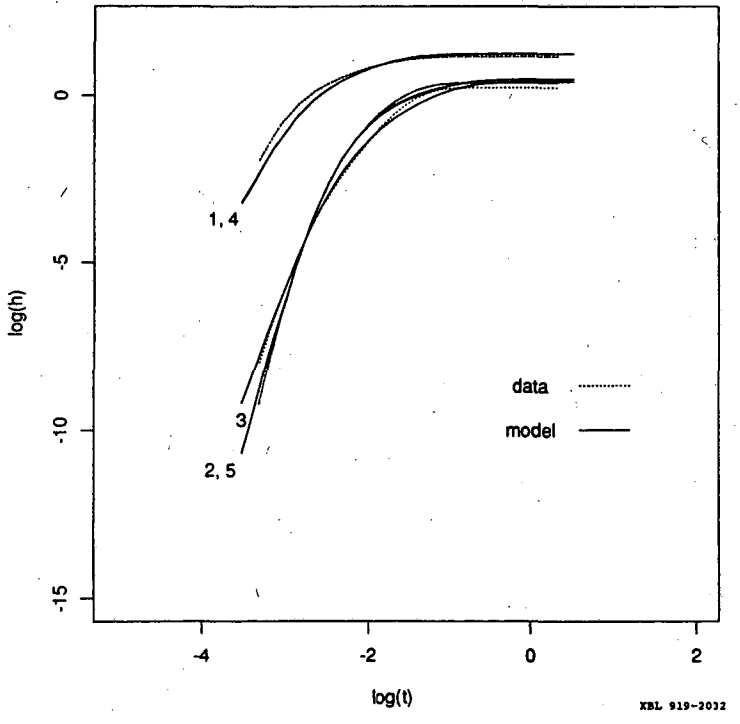

Figure 5.7. Transient drawdown responses for the second synthetic case for the low conductivity in the center.

6.0 INVERSION OF DATA FROM HETEROGENEOUS POROUS MATERIALS

A variety of well tests have been conducted on a shallow aquifer system composed of interbedded sands, silts, and clays at Kesterson Reservoir, located in the San Joaquin Valley in central California (Yates, 1988). The hydrological properties of the aquifer/aquitard system are needed in order to study the transport of various forms of selenium and other salts between surface waters and underlying aquifers. The aquifer studied in the present example is about 18 m thick, and is underlain by an impermeable clay layer and overlain by a leaky aquitard. A multi-well transient pump test is analyzed to infer the spatial distribution of permeability in the aquifer.

In the test under consideration, a central well was pumped at a constant rate and, transient drawdowns were measured at eight observation wells located 15 to 107 m away from the pumping well (see Figure 6.1a). A two-dimensional areal finite element model is used to represent the aquifer.

Figure 6.2 shows the observed drawdown vs. time curves and those calculated assuming a medium with uniform conductivity and storativity (no attractor). The energy of the uniform-medium solution is E = 38.

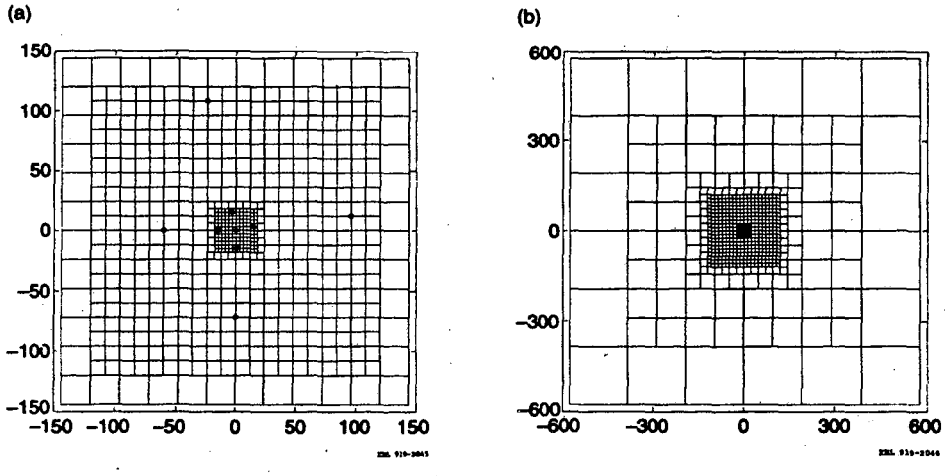

Figure 6.1. The two-dimensional finite element mesh used for the Kesterson calculation. Frame (a) shows the central part of the mesh with the well field superposed, frame (b) shows the entire mesh.

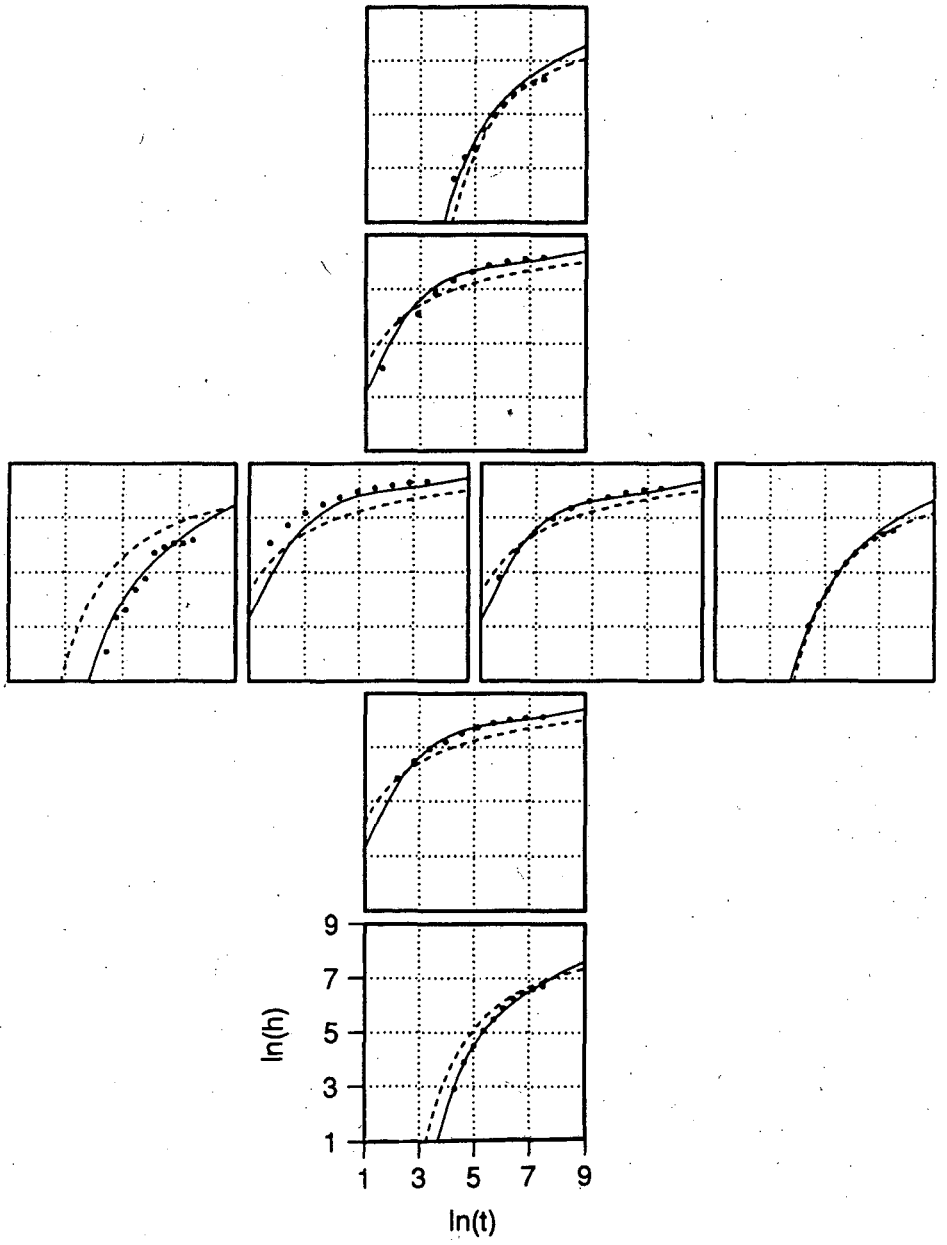

Figure 6.2. The transient drawdown response in the Kesterson observation wells: observed data (black dots), calculated response assuming a uniform medium (dashed lines, E = 38), and the calculated response that produces the minimum energy (solid lines, E = 6). The arrangement of the plots on the page follows the locations of the observations wells in the well field (Figure 6.1a).

During the inversion the attractor is constrained to remain within the region $|x| < 150$, $|y| < 150$ m shown in Figure 6.1a. If this constraint is not included, the inversion tends to waste effort changing the attractor far from the well field, where changes have little impact on the observed drawdowns. Each point of the attractor increments the conductance of the nearest mesh element. The final attractor resulting from the inversion is shown in Figure 6.3. The drawdown vs. time curves for this attractor are shown in Figure 6.2 and correspond to an energy of E = 6.

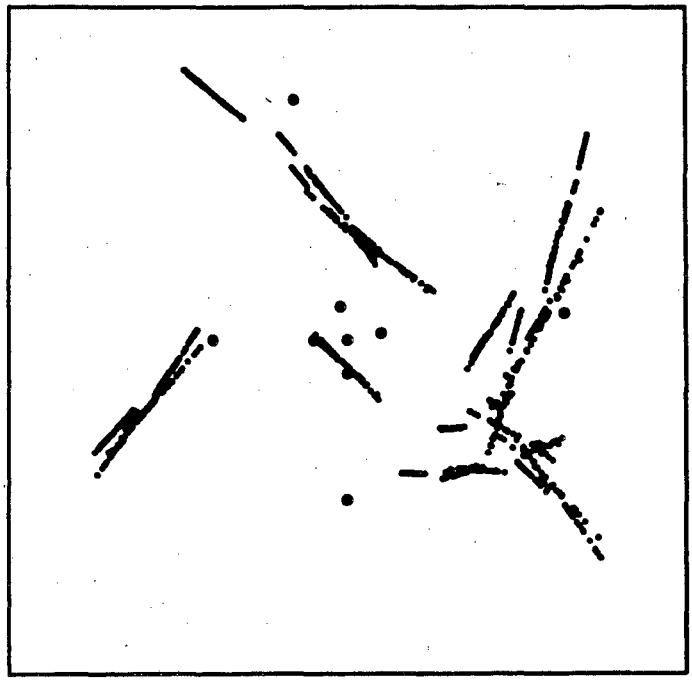

XBL 924-782

Figure 6.3. The attractor that yields the minimum energy (E = 6) for the Kesterson data.

In conclusion, the inverse method has worked well to match the observed head data. However, we have used a two-dimensional model for a three-dimensional problem, and in so doing may have obscured the effects of some geologic heterogeneities and not represented leakage from over and underlying strata.

To correctly analyze this well test, we should use a three-dimensional conceptual model. The IFS inversion method can be easily applied to these dimensions, but the computational effort will be greatly increased. Not only will the flow problem require far more computational time due to larger meshes, but a general three-dimensional attractor has 12 parameters for each affine transformation, compared to 6 for a two-dimensional attractor, doubling the dimension of

the parameter space that must be searched by the inversion. Never the less, large three-dimensional inversions have been successfully computed using Simulated Annealing and it is well within the realm of possibility to perform three-dimensional IFS inversions.

7.0 INVERSION OF DATA FROM FRACTURED ROCK

At the Stripa mine in Sweden, we have been investigating the hydrology of a subvertical fracture zone called the H-zone within a 150 m × 100 m × 50 m block of rock. A series of seven wells (C1, C2, C3, C4, C5, W1, W2) penetrate this zone. An interference test, called the C1-2 test, was conducted in these holes. In this test, the C1 hole was pumped at a constant rate from a packed-off interval (interval 2) in the H-zone. Responses were measured in the other holes in intervals packed-off around the H-zone. A second experiment, called the Simulated Drift Experiment (SDE), measured the steady-state flow rate from the H-zone into an additional six parallel holes drilled within a 1 m radius (the D-holes). The entire data set is described in Olsson et al. (1989) and Black et al. (1991). An inversion of this data using Simulated Annealing is given in Long et al. (1991).

Here we present an IFS inversion based on the C1-2 cross-hole test. We then use the model produced by the inversion to predict the flow rate into the D-holes in the SDE. We treat the H-zone as a two-dimensional feature. The C-, D-, and W-boreholes penetrate the plane of the H-zone. The IFS on the plane of the H-zone describes the high conductivity regions within the plane of the fracture zone.

We first find an IFS which creates a hydrologic property distribution that reproduces the C1-2 interference data, in which a constant-flow boundary condition is applied at the C1 hole. Then we use this model to calculate the steady-state inflow to the SDE, in which a constant drawdown is imposed at the D-holes.

A two-dimensional variable-density mesh was used to model the H-zone, in order to maximize detail in the vicinity of the D-holes, provide a large enough mesh to prevent the transients from reaching the boundary too soon, and minimize the number of elements and bandwidth. The outer boundary conditions in the model were chosen to represent the estimated equilibrium head values.

7.1 IFS Inversion Based on C1-2

The inversion was done using three affine transformations in which each point on the attractor incremented both the conductance and the storativity of the nearest element. Figure 7.1 shows the well test data and the model results for the 799th iteration where the energy had dropped to about E = 13 from an initial value of about E = 45. Figure 7.2 shows the attractor at iteration 799.

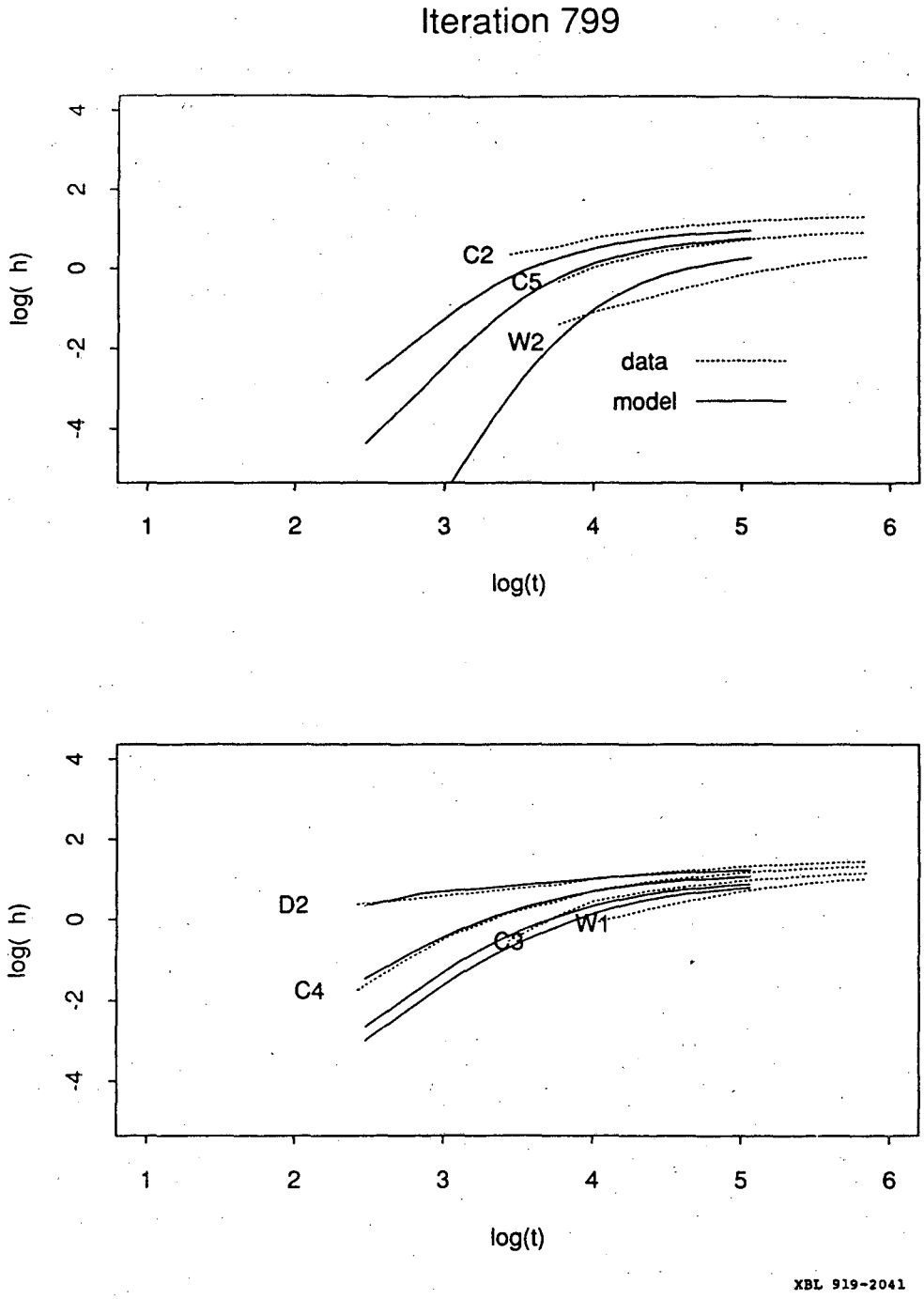

Figure 7.1. The well test data from the Stripa C1-2 test compared to the model results for iteration 799.

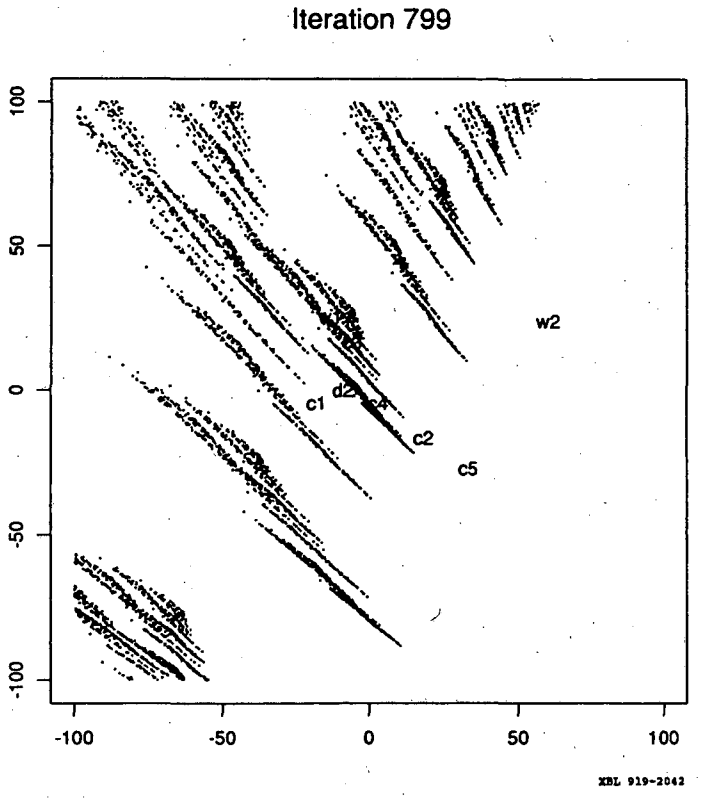

Figure 7.2. The attractor found at iteration 799 for the central 200 × 200 m section of the mesh. The six D-holes are in the immediate vicinity of D_2.

7.2. Prediction of Flow for the Simulated Drift Experiment (SDE)

We then predicted the flow rate into the D-holes during the SDE by applying a constant head at the D-holes such that we impose the same drawdown at the D-holes (220 m) as was imposed during the SDE. The actual flow rate to the D-holes from the H-zone during the SDE was estimated to be about 0.7 l/min. Our calculation gives 0.4 l/min which is low, but reasonably close.

Some interesting attributes of this inversion are that the attractor first resided entirely in the upper left-hand corner of the mesh and consistently migrated to the lower right with each iteration. Thus, the conductance in the vicinity of the C- and D-holes consistently increased, which means that further iterations may continue to move the attractor down and improve the solution. However, another possibility is that we are using too many points in the attractor which results in too high a conductance contrast, effectively forcing the attractor to stay away from the center of the well field. These possibilities are under investigation.

8.0 ITERATED FUNCTIONS TO DESCRIBE FRACTURE PATTERNS (JOINTS)

One exciting possibility for IFS inversion is that we may be able to condition the inversion on geologic information. If we can find Iterated Function Systems that reproduce the geometry of a geologic system, then inversion searches could be restricted to this class of functions. Probably the best way to find such classes of iterated functions is to base the functions on an understanding of how the system in question develops. For example, a meander belt might be described based on a physical understanding of its depositional history. For a set of joints, the functions could reflect the growth mechanics of the joints. A preliminary example of such a description of joint growth is given below.

The IFS scheme considered here is stochastic but is based on fracture mechanics concepts. The cases we consider pertain to two-dimensional fracture growth in homogeneous, isotropic elastic materials under plane strain conditions.

A commonly used criterion for fracture propagation is that fracture growth will be in the direction that minimizes the energy release rate G. For the two-dimensional case considered here

$$G = (K_I^2+K_{II}^2)\frac{1-\nu^2}{E} \tag{8.1}$$

where K_I and K_{II} are the mode I and mode II stress intensity factors, respectively (Lawn and Wilshaw, 1975). The terms ν and E are elastic constants: ν is Poisson's ratio, and E is Young's modulus. For an isolated mode I crack (dilatant fracture or joint), K_{II} equals zero and

$$K_I = \sigma_d\sqrt{\pi L/2} \tag{8.2}$$

where σ_d is the driving pressure and L is the length of the crack. Expressions (8.1) and (8.2) together show that

$$G \propto L. \tag{8.3}$$

According to classical fracture mechanics, a fracture subject to a constant driving pressure will grow rapidly if G exceeds a critical level, G_c, which is a material property. By this criterion, once a fracture reaches a critical length it should continue propagating with no increase in the driving pressure. Subcritical (slow) fracture growth can occur if G is below G_c. The subcritical fracture growth rate v is commonly described by a power law, $v \propto G^n$, (Atkinson and Meredith, 1987a). Although experimental values of the exponent n usually exceed 10 (Atkinson and Meredith, 1987b), Olson (1990) argues that field evidence suggests that n commonly is near 1 under natural conditions. If so, this would mean that $v \propto L$ for subcritical growth.

We assume that the relative probability of fracture growth (either by propagation of an existing fracture or by growth of a new "daughter fracture" near the tip of a pre-existing parent) is proportional to G. Based on Equation (8.3) we

scale the relative growth probabilities to the fracture length L:

$$P_1(\text{fracture growth}) \begin{cases} =(1/L_c)\,L & L < L_c \\ =1 & L \geq L_c \end{cases} \tag{8.4}$$

The constant of proportionality ($1/L_c$) acts as a critical length in Equation (8.4). During a given iteration through the fracture-generating program, growth *will* occur for fractures longer than L_c. Growth *may* occur for fractures shorter than L_c; this condition corresponds to subcritical crack growth.

The IFS algorithm proceeds in four steps, with each fracture checked in a given iteration. First, a decision is made regarding fracture growth. The probability of fracture growth P_1 is calculated using Equation (8.4), and a random number Q_1 between 0 and 1. If P_1 is greater than Q_1, there will be growth; if not, another fracture is checked for growth. Second, a decision is made whether the pre-existing "parent" will grow or a new "daughter" crack will form. The parameter that defines the relative probability of in-plane propagation of a parent is P_2; the relative probability of a daughter nucleating is therefore $(1\text{-}P_2)$. Another random number Q_2 between 0 and 1 is selected. If P_2 is greater than Q_2, the parent will grow; otherwise, a daughter will form. Third, the increment of growth ΔL is calculated according to the expression

$$\Delta L = LBQ_3 \tag{8.5}$$

where L is the parent length, B is a maximum growth increment parameter set by the user ($0 < B < 1$), and Q_3 is a random number between 0 and 1.

Fourth, if a daughter crack forms, its location must be determined. The coordinates (r,θ) of the center of a daughter crack are set relative to the tip of the parent crack (Figure 8.1). They are determined stochastically using two random numbers (Q_4 and Q_5) and a probability density distribution based on the stress state near a crack tip. The equation for the crack-perpendicular stress (σ_{yy}) near the tip of a crack is (Lawn and Wilshaw, 1975):

$$\sigma_{yy}(r,\theta) = (K_I/\sqrt{2\pi r})\cos(\theta/2)[1+\sin(\theta/2)\cos(3\theta/2)] \tag{8.6}$$
$$-\pi < \theta < \pi, \quad 0 < r < B$$

The contributions that contain r and θ in Equation (8.6) can be isolated and normalized to yield probability density distributions for daughter crack locations as a function of r and θ. These distributions show that the probability density tails off with distance from the crack tip and has maxima near $\theta = \pm 60°$ instead of directly ahead of the crack tip. This causes a daughter crack to preferentially grow near the tip of a parent crack but off to the side.

The number of iterations through the algorithm is set by the user. A larger number of iterations allows longer and more numerous fractures to be grown.

There are four key aspects of this approach that should make it useful. First, it can generate fracture patterns in much less time than approaches that explicitly account for the mechanical interaction between fractures. Second, fracture

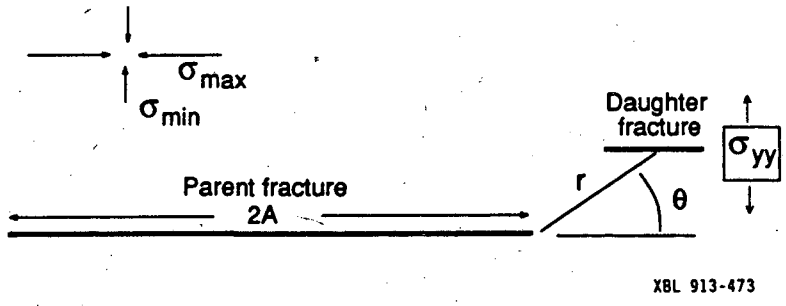

Figure 8.1. Diagram showing the relative positions of a parent fracture and a daughter fracture and the orientations of the most-compressive and least-compressive far-field stresses.

growth occurs only near crack tips (where stresses are particularly favorable), so in this regard it is consistent with fracture mechanics principles. Third, new cracks can develop; techniques that explicitly account for fracture interaction usually only allow pre-existing fractures to grow. Fourth, there are only a few parameters to manipulate (the starter crack distribution, P_2, B, L_c, and the number of iterations).

An important assumption incorporated in the rules outlined above is that fracture interaction is weak and that every crack grows as though it were isolated. As a result the algorithm only permits a parallel set of fractures to grow. This approach most appropriately applies to cases where the far-field principal stresses (rather than crack interactions) dictate fracture shapes and the stress perturbations due to fracture interaction are weak (i.e. the difference in magnitude between the remote principal stresses is large relative to the driving pressure in the fractures; driving pressure equals internal fluid pressure minus remote least compressive principal stress). Although this is a significant restriction, it should not invalidate the approach. The fracture traces in many natural sets are fairly straight, indicating that fracture interaction commonly is not strong.

From the simulations conducted to date, three main points emerge. First, this approach can generate realistic-looking fracture growth sequences (Figure 8.2) that compare favorably with detailed outcrop maps (e.g. Figure 8.3). Second, many starter cracks are needed to produce realistic-looking patterns. Third, most realistic-looking patterns are produced if the probability of daughter fracture generation is very low. If $P_2 = 1$ (i.e. only pre-existing cracks can grow) and the length of the starter cracks is is greater than L_c, then the resulting fracture length distribution approaches a log-normal distribution as the number of iterations becomes large (Figure 8.4). Even a very small probability of daughter growth can cause a tremendous change in the fracture length distribution. Figure 8.4 also shows a distribution produced when the probability of daughter growth $1-P_2 = 0.01$. This distribution would be better described by a power-law function. For cases such as this, the shortest cracks are concentrated in belts along the largest fractures. This type of pattern resembles joint zones.

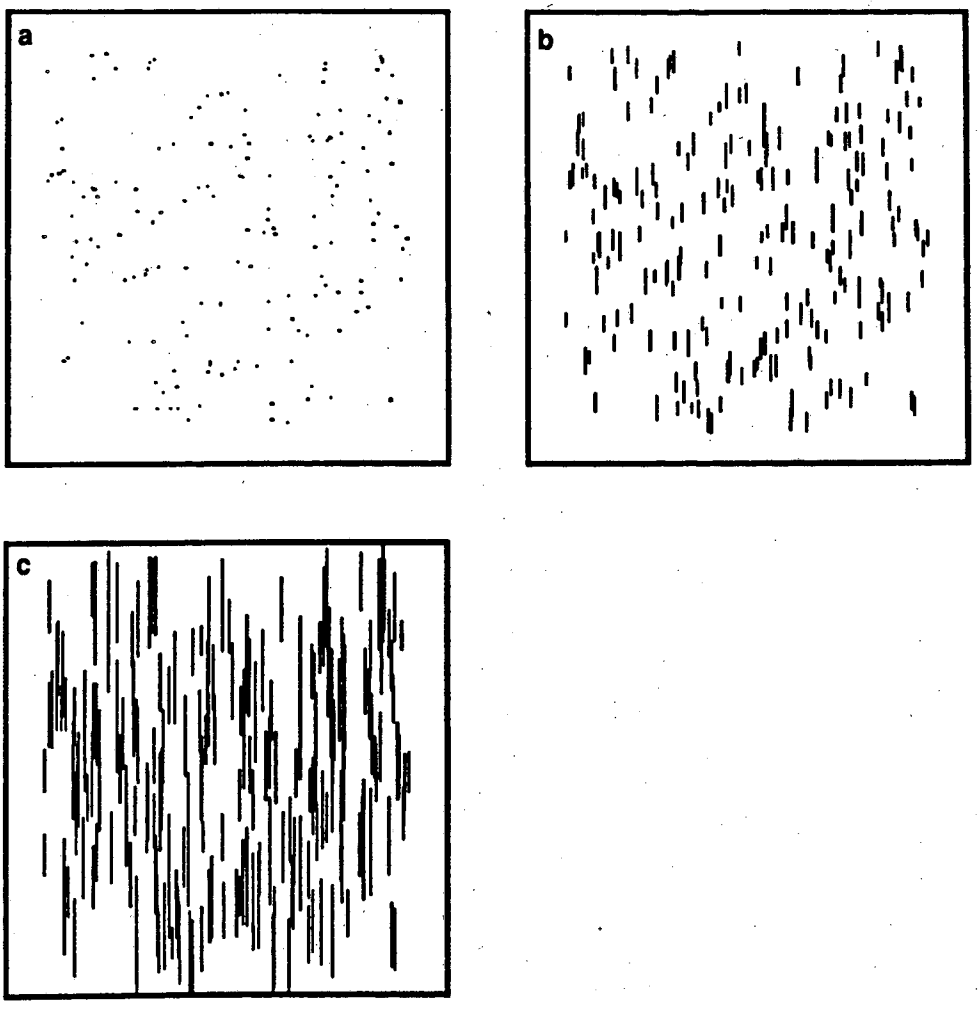

XBL 919-2043

Figure 8.2. Development of a fracture pattern from 200 randomly located starter cracks after (a) 0, (b) 110, and (c) 140 iterations. Each starter crack in (a) is 1 cm long, a distance corresponding to the likely initial crack length of Figure 8.3.

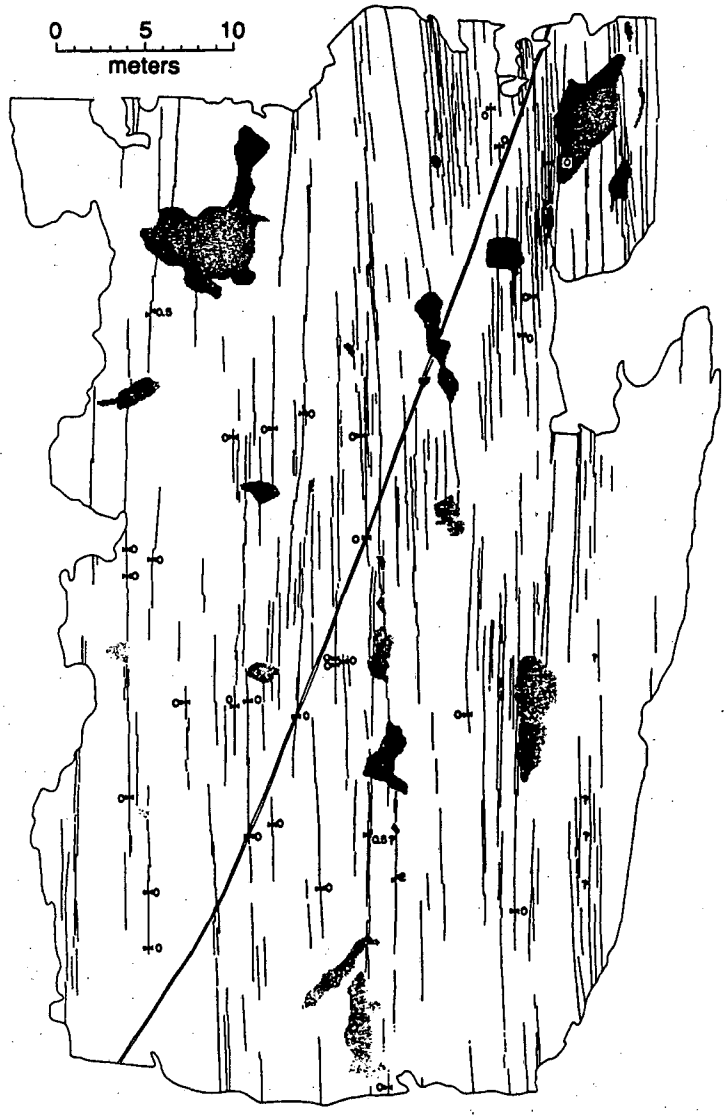

Figure 8.3. Map of fracture traces in a granite outcrop (modified from Segall and Pollard, 1983). The fractures dip steeply. Numbers indicate amount of lateral separation (in centimeters) across fractures. The feature marked by a double line is vein. Areas where the outcrop is covered are shown in gray. The pattern here is visually similar to that in Figure 8.2c.

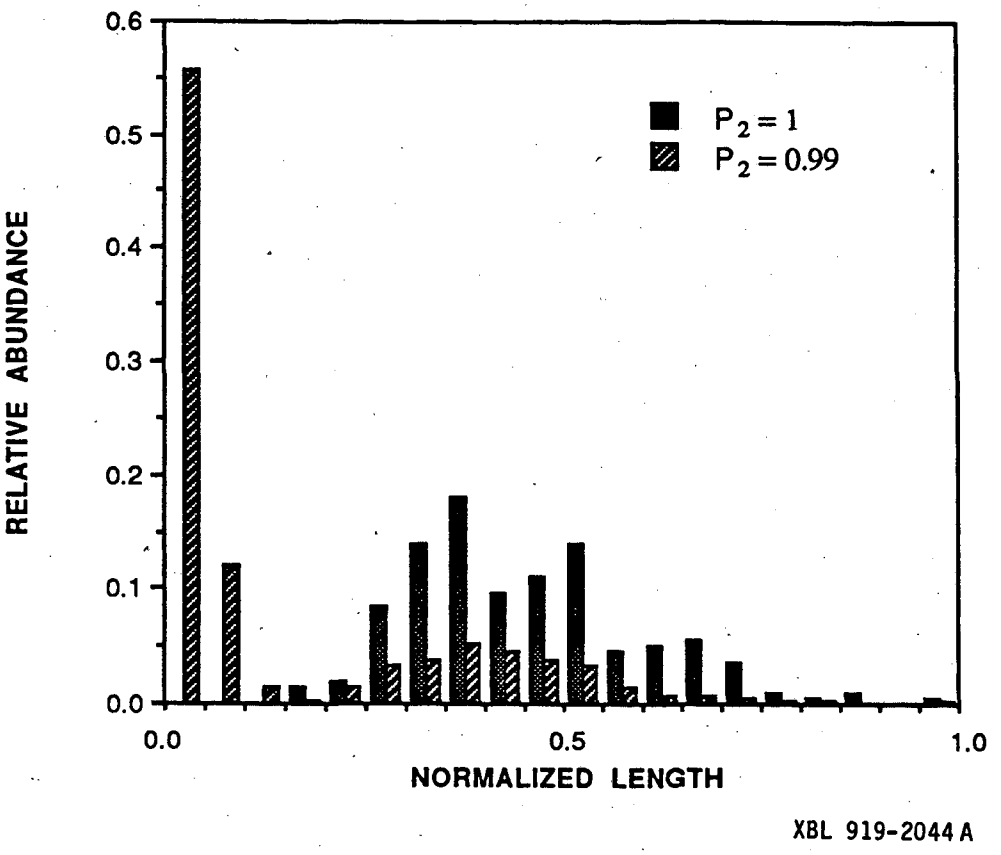

Figure 8.4. Comparison of two fracture length distributions developed from 200 starter cracks and 150 iterations. For P_2 = 1.0 the distribution is approximately lognormal; for P_2 = 0.99 the distribution is better described by a power law. Fracture lengths are normalized by the longest fracture length.

9.0 CONCLUSIONS AND RECOMMENDATIONS

This paper gives some preliminary applications of a new inverse approach to modeling heterogeneous and fractured reservoirs. We believe this approach has great possibilities as a practical tool. However, to reach this goal, much remains to be done. We need to learn more about how the inversion process works. The techniques we have started with could be extended to apply to more complex cases and data sets. To do this we will have to improve the "intelligence" of the search for good solutions. In the real world, where we never know enough about the subsurface environment, this method can provide a series of comparable solutions that reproduce the behavior we know about and extend our abilities to predict behavior in the future. Below, we discuss these points.

9.1 The Inversion Algorithm

We are just beginning to see how the inversion algorithm works. The technique has a strong scientific basis, but at this point the application requires arbitrary decisions. We need to begin to dissect these decisions to see how they affect the solutions. For example, we assign changes in conductance to the elements of the background lattice in an arbitrary way. We have chosen to increment conductance but if, for example, we are looking at clay lenses in sand, we might want to decrement conductance. In some cases we only incremented the element nearest the attractor point, in other cases we proportioned the increment according to proximity to the point in order to produce a smoother distribution. Different geologic systems may provide a reason for doing one or the other. The way in which we assign conductance increments will effect the resolution of anomalous features.

We also connect the increment in conductance to an increment in storativity. These two parameters are not necessarily uniquely related and we might need to determine when a more complex relationship is required. For example, clays may have high storativity and low conductance, whereas the opposite can hold for sands. We might have to define several conductivity and storativity relationships and a set of rules for using one or the other. Similarly, we arbitrarily choose M, the number of points in the attractor. We could begin to include this parameter in the inversion, possibly by stopping the process after a certain number of iterations, optimizing M and then continuing, etc.

9.2 Extensions of the Method

At the present time we are able to look at two-dimensional systems and invert based on either one steady or transient well test. Obvious extensions include the ability to include more than one well test simultaneously. Preliminary work with Simulated Annealing indicated that predictions based on two well tests significantly improved over those using one. Adding more well tests is analogous to increasing the ray coverage in producing a geophysical tomogram.

Although we have never run a fully three-dimensional IFS inversion, there is in principle nothing preventing us from doing so even though it may be time consuming. For example, we might model the Kesterson case as several layers and in this way be able to include some of the partial penetration and leakage effects that we have had to neglect in our two-dimensional model.

Use of diffusive phenomena such as pressure transients to resolve permeability anomalies has some inherent difficulties. When we receive a pressure transient, we commonly have little idea of the geometry of the flow path between the source and the observation. The fact that this path may be significantly different than a straight line means that the pressure transient data is inherently hard to interpret. One might say that the information in the signal is "diffused." This fact has always pointed to the use of tracer tests as an alternative data source for inversion. This is under consideration, but will probably introduce as many

complications as it removes. It is probably true that one can do better predicting head by inverting head measurements, predicting flow by inverting flow measurements, and predicting tracer arrival times by inverting arrival time measurements. The task of building one model that can predict all of these simultaneously is a research program in itself.

9.3 Efficiency

Clearly if we want to make IFS inversion a practical tool we must find efficient algorithms. The inversions done for this paper were completed with very crude, simple codes which in no way optimized the calculations. They were run on a Solbourne 500 series workstation, with CPU times ranging from 25 minutes for the first synthetic case (which was specifically designed to run quickly) to about two days for the Kesterson inversion.

The computer science aspects of this problem are important. These can include simply better programming and optimization algorithms, but might also include the use of chip design such that the relevant equations are hard-wired into the computer. Solvers based on computer architecture are very attractive for these problems where we expect to make many thousands of iterations. Another interesting possibility is to learn to solve the diffusion equation analytically directly on the attractor, thus obviating the need for extensive numerical analysis of each iteration.

A more down to earth way to improve efficiency is to be smarter about the way that we search for solutions. We can incorporate *a priori* information such as geophysical data to force the search to look for permeability anomalies where there are geophysical anomalies. This is conceptually very simple and could be incorporated very easily simply by lowering the energy when an attractor point falls inside the geophysical anomaly. Co-inversion of both geophysical data and hydrologic data might be useful, but our experience is that it may be better to use the interpretation of the geophysical results as *a priori* information in the hydrologic inversion. This is because a significant amount of expert judgment is called on to interpret geophysical measurements and this judgment would be overlooked in a co-inversion.

9.4 Geologic Approach

The work on fracture growth schemes has tremendous promise for being able to reproduce fracture patterns. Clearly, similar work could be done to describe other hydrologically important geologic features. Sites which have been exhaustively explored will be critical for learning to build functions that describe heterogeneities for specific geologic conditions. Several such sites are being developed for the purpose of understanding heterogeneity and may be very useful for this work.

The work on graphics using Iterated Function Systems has included development of techniques for finding the IFS that describes a given pixel plot. This work could be extended to three-dimensions in order to find the IFS that

describes the geology of a given quantified site. If we can then begin to examine the nature of these functions, we may characterize classes of IFS that represent geologic situations.

If hydrologic inversions can be limited to geologically determined classes of Iterated Function Systems, this would produce results that à priori resolve realistic features. In this way it may be possible to improve the efficiency, resolution and extrapolation of hydrologic inversions.

9.5 Uniqueness and Prediction

The problem of specifying the uniqueness of solutions always arises in the inverse problem, especially in the earth sciences. The fact is that we rarely if ever have enough data to completely specify an underground system and we have to accept uncertainty. What is especially attractive about the IFS inverse approaches we are developing is that they produce a range of solutions and thus can produce a range of predictions.

We think it is important to design approaches to the reservoir characterization problem that recognize from the beginning that the solution to the inverse problem is non-unique and that predictions made with these models have errors which should be quantified in some way. A good research program in reservoir characterization should include a sequence of predictions and measurements in order to determine if the model is converging to a useful predictive tool. A simple example of this would be to use an inversion based on one well test to predict the results of a second; then the two tests to predict the results of a third, etc. In this way we can see how much data is needed to make predictions sufficient for the purpose at hand.

9.6 Evaluation

The IFS inversion scheme seems to be a promising line of research. The approach is inherently interdisciplinary in nature and should be able to produce models that incorporate the many types of information that are available for a reservoir. The models use behavior to predict behavior and are consequently inherently consistent. Some encouraging initial results have been obtained, but there is much left to do.

10.0 REFERENCES

Atkinson, B. K., and Meredith, P. G., 1987a. The Theory of Subcritical Crack Growth with Applications to Minerals and Rocks, *Fracture Mechanics of Rock,* Atkinson, B. K., ed., Academic Press, London, p. 111-166.

Atkinson, B. K., and Meredith, P. G., 1987b. Experimental Fracture Mechanics Data for Rocks and Minerals, *Fracture Mechanics of Rock,* Atkinson, B. K., ed., Academic Press, London, p. 477-525.

Barnsley, M., 1988. *Fractals Everywhere,* Academic Press, Inc., Boston, Ch. 3.

Black, J. H., Olsson, O., Gale, J. E., Holmes, D. C., 1991. Site Characterization and Validation, Stage 4, Preliminary Assessment and Detail Predictions, Report in preparation, Swedish Nuclear Fuel and Waste Management Co., Stockholm, Sweden.

Carrera, J. and Neuman, S. P., 1986a. Estimation of Aquifer Parameters under Transient and Steady State Conditions: 1. Maximum Likelihood Method Incorporating Prior Information, *Water Resources Research, 22,* (2), 199-210.

Carrera, J. and Neuman, S. P., 1986b. Estimation of Aquifer Parameters under Transient and Steady State Conditions: 2. Uniqueness, Stability, and Solution Algorithms, *Water Resources Research, 22,* (2), 211-227.

Carrera, J. and Neuman, S. P., 1986c. Estimation of Aquifer Parameters under Transient and Steady State Conditions: 3. Application to Synthetic and Field Data, *Water Resources Research, 22,* (2), 228-242.

Davey, A., Karasaki, K., Long, J. C. S., Landsfeld, M., Mensch, A. and Martel, S. 1989. Analysis of the Hydraulic Data of the MI Experiment, Report No. LBL-27864, Lawrence Berkeley Laboratory, Berkeley, California.

Freeze, R. A., 1975. A Stochastic-Conceptual Analysis of One-Dimensional Groundwater Flow in Nonuniform Homogeneous Media, *Water Resources Research, 11,* (5), 725-741.

Karasaki, K, 1987. A New Advection-Dispersion Code for Calculating Transport in Fracture Networks, Earth Sciences Division 1986 Annual Report, LBL-22090, Lawrence Berkeley Laboratory, Berkeley, California, pp. 55-58.

Kitanidis, P. K. and Vomvoris, E. G., 1983. A Geostatistical Approach to the Inverse Problem in Groundwater Modeling (Steady State) and One-Dimensional Simulations, *Water Resources Research, 19,* (3), 677-690.

Lawn, B. R. and Wilshaw, T. R., 1975. *Fracture of Brittle Solids,* Cambridge University Press, 204 pp.

Long, J. C. S., Mauldon, A. D., Nelson, K., Martel, S., Fuller, P. and Karasaki, K, 1991. Prediction of Flow and Drawdown for the Site Characterization and Validation Site in the Stripa Mine, Report No. LBL-31761, Lawrence Berkeley Laboratory, Berkeley, California.

Olson, J. E., 1990. Fracture Mechanics Analysis of Joints and Veins, Stanford University, Stanford, California [Ph.D. dissertation], 187 pp.

Olsson, O., Black, J. H., Gale, J. E. and Holmes, D. C., 1989. Site Characterization and Validation, Stage 2, Preliminary Predictions, Report TR 89-03, Swedish Nuclear Fuel and Waste Management Co., Stockholm, Sweden.

Press, W. H., Flannery, B. P, Teukolsky, S. A., Vetterling, W. T., 1986. *Numerical Recipes: The Art of Scientific Computing,* Cambridge University Press, New York, Ch. 10.

Segall, P., and Pollard, D. D., 1983. Joint Formation in Granitic Rock of the Sierra Nevada. *Geological Society of America Bulletin, 94*, 454-462.

Toth, J., 1967. Groundwater in Sedimentary (Clastic Rocks). Proc. National Symposium on Groundwater Hydrology, San Francisco, CA, Nov. 6-8, p. 91-100.

Yates, C. C., 1988. Analysis of Pumping Test Data of a Leaky and Layered Aquifer with Partially Penetrating Wells, University of California, Berkeley [M.Sc. dissertation], 198 pp.

ACKNOWLEDGMENT

The fracture related work was supported by the Director, Office of Civilian Radioactive Waste Management, Office of External Relations and and the porous media work was supported by the Office of Health and Environmental Research, Ecological Research Division, Subsurface Science Program at the Lawrence Berkeley Laboratory which is operated by the University of California under U. S. Department of Energy Contract No. DE-AC03-76SF00098. The authors are grateful to Robert Zimmerman and Ernest Majer for their thoughtful reviews.

LAWRENCE BERKELEY LABORATORY
UNIVERSITY OF CALIFORNIA
TECHNICAL INFORMATION DEPARTMENT
BERKELEY, CALIFORNIA 94720